Organic Thin-Film Transistors Fabricated on Resorbable Biomaterial Substrates

By *Christopher J. Bettinger* and *Zhenan Bao**

Microelectronic systems utilizing organic materials show many advantages over traditional silicon-based systems. Organic electronic devices have potential manufacturing advantages including solution processing and large-scale fabrication with reduced cost. Furthermore, organic devices can be easily fabricated on polymeric substrates, which are suitable for a broad range of applications in flexible electronics including conformal devices and displays, and are also potentially suitable for roll-to-roll fabrication strategies. For example, many types of organic devices, including transistors, sensors, and photovoltaic cells, have been fabricated on both natural and synthetic flexible polymers including poly(ethylene terepthalate),[1–3] poly(imide),[4] poly(ether sulfone),[5] cellulose,[6,7] and silk fibroin.[8] Various organic polymeric systems composed of biodegradable polymers[9] have demonstrated utility in many applications including temporary medical implants[10,11] and compostable products.[12] For example, thermoplastic polyesters such as poly (L-lactide-*co*-glycolide) (PLGA) are a commonly used biodegradable polymer for drug-delivery systems and medical implants, while poly(4-hydroxybutyrate) (P4HB) is commonly used as a biodegradable plastic for disposable products.[13] Water-soluble polymers such as dextran and poly(vinyl alcohol) (PVA) have been used for a variety of biomedical applications including tissue-engineering scaffolds[14] and environmental applications.[15] Recent progress in the design and synthesis of organic semiconductors have led to the realization of molecules that can operate stably in hydrated or oxidative environments,[16] including p-channel materials based on thiophenes[17] or fluorenes[18] and n-channel materials based on perylene diimides.[19] These concomitant advancements in organic electronics and biodegradable-polymer processing suggest that there is potential for the use of biodegradable polymeric systems and the development of biodegradable electronic devices for potential use in biomedical or environmental applications. Toward this end, we investigated materials and fabrication strategies for the realization of organic thin-film transistor using a small-molecule semiconductor in combination with a biodegradable polymeric substrate and dielectric. We demonstrate that these devices perform stably after exposure to water and, since they consist of nearly entirely biodegradable materials, these devices are resorbable in an in vitro degradation environment.

A schematic image of the device is shown in Figure 1. The strategy for material selection focused on utilizing materials that are biocompatible and biodegradable, yet also exhibit adequate electronic properties and suitable device processing capability. The biomaterials selected for the substrate and dielectric layer should exhibit a unique intersection of biological and electronic properties that is compatible with a variety of polymer processing techniques. From a biomaterial perspective, the materials should be resorbable, exhibit excellent biocompatibility profiles, and, ideally, have been previously utilized in biomedical devices that have been approved by the United States Food and Drug Administration (FDA). The polymers should be soluble in orthogonal solvent systems to promote facile processing methods including casting and spin-coating. These constraints on material properties led to the selection of PLGA and PVA polymers to be used as the substrate and gate dielectric in the device, respectively. PLGA and PVA polymers are inexpensive, commercially available, and have been previously used in a wide array of biomedical devices for clinical applications.

The semiconducting molecule utilized in this study consists primarily of a large core consisting of conjugated substituents.

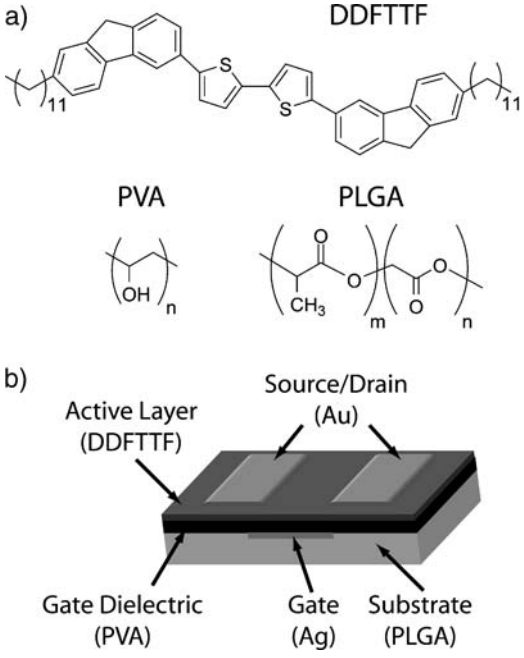

Figure 1. Materials selection and device configuration of organic thin-film transistors. a) The chemical structures of the semiconductor (DDFTTF), the dielectric (PVA), and the substrate (PLGA) are shown. b) These materials are processed into devices in top-contact configuration as shown. Briefly, PLGA was melt-processed into substrates ~1 cm × 1 cm in area and 2 mm in thickness. Silver gate contacts were evaporated through a shadow mask. PVA dielectrics were spin-coated from solution followed by thermal evaporation of DDFTTF semiconducting layers and gold source/drain contacts. The final device geometry contained channel lengths of 50 μm and a *W*/*L* ratio of 20.

[*] Prof. Z. Bao, Dr. C. J. Bettinger
381 North South Mall, Stauffer III, Room 113
Stanford, CA 94305-5025 (USA)
E-mail: zbao@stanford.edu

DOI: 10.1002/adma.200902322

Table 1. Summary of the device performance of DDFTTF-based transistors on PVA dielectrics with PLGA substrates. Devices fabricated on nPVA exhibited higher mobilities, higher on/off ratios, and smaller threshold voltages compared to devices fabricated on xPVA. Frequency distributions are shown in Figure S3.

Dielectric Material	Dielectric Constant, k	Capacitance, C_d [nF cm^{-2}]	Mobility, μ [cm^2 sec^{-1} V^{-1}]	Threshold Voltage, V_T [V]	On/Off Ratio, I_{on}/I_{off}
nPVA	7.6	5.20	0.207 ± 0.069	-15.4 ± 1.7	$5.5 \pm 2.1 \times 10^3$
xPVA	6.7	4.56	0.057 ± 0.018	-18.9 ± 4.9	$3.2 \pm 0.69 \times 10^3$

5,5′-bis-(7-dodecyl-9*H*-fluoren-2-yl)-2,2′-bithiophene (DDFTTF). DDFTTF is a robust small-molecule p-channel semiconductor that exhibits excellent device performance and is resistant to harsh environments including aqueous conditions.[17] Although the biodegradation of DDFTTF has not been explicitly studied, degradation mechanisms that are used to decompose melanin,[20,21] a conjugated amorphous semiconductor,[22,23] could potentially be expanded in a similar manner to DDFTTF. Therefore, we elected to deposit DDFTTF as the active layer through thermal evaporation. The choice of conducting metals for electrical contacts was based primarily on process considerations, yet both are potentially suitable for use in medical devices. Silver exhibits suitable biocompatible properties in vitro and in vivo and has been used as an antimicrobial agent in biomedical implants for a variety of clinical applications.[24,25] Gold is an inert biomaterial that exhibited reduced biofouling in vivo for various biomedical implants including cardiovascular[26] and BioMEMS devices.[27]

The substrate, which composes 99.89% of the total mass of the device, was chosen to consist of PLGA, a linear biodegradable thermoplastic polyester. PLGA with a high relative amount of lactic acid was chosen (PLGA 85:15) because of the elevated glass-transition temperature, T_g, which allows for processing at elevated temperatures. The surfaces of melt-processed PLGA substrates were extremely smooth with root mean square (rms) roughness of 0.46 nm, which facilitated subsequent device fabrication. However, the physical properties of thermoplastic PLGA provided limitations in downstream device processing due to: (i) low melting point (T_m) and T_g and (ii) solubility in common organic solvents. These properties suggest the use of mild downstream processing conditions and the use of water-soluble PVA as a solution-processable dielectric, respectively. PVA is a water-soluble, environmentally biodegradable polymer[15] that has also demonstrated reasonable utility in organic electronics.[28] PVA exhibits a large dielectric constant and is processable into thin films with a small free volume. These properties would ultimately serve to reduce operating voltages and gate leakage currents. PVA also has the ability to be photocrosslinked by incorporating ammonium dichromate (ADC) and irradiating films with UV light, which enables the possibility of photolithographically defined features. High-molecular-weight electrical grade PVA ($M_w \sim 205000$ Da) was processed into relatively thick PVA films (1.3 μm) for two primary reasons: (i) to reduce the gate-leakage current and (ii) to mask this roughness and prevent electrical short defects between gate and source/drain electrodes. Despite relatively lower capacitance values, PVA dielectrics on the order of 1 μm have been shown to serve as effective dielectric layers (Table 1).[29,30] Noncrosslinked PVA (nPVA) and photocrosslinked PVA (xPVA) films exhibited rms roughness values of 0.31 and 0.24 nm, respectively.

DDFTTF films evaporated at 50 °C on both nPVA and xPVA exhibited island morphologies with extremely high aspect-ratio features (Fig. S1 of the Supporting Information). Enhanced performance is observed in DDFTTF if the substrate is maintained at ~95 °C during deposition.[17] However, the maximum substrate temperature that could be achieved using PLGA substrates was nominally 50 °C. The lower temperature could lead to reduced transistor performance relative to previous studies.[17] This resulted in rough films with rms-roughness values of 21.14 and 19.45 nm, respectively. Conductive gate electrodes fabricated through rapid thermal deposition of silver enabled the formation of films nominally 15–20 nm in thickness without macroscopic defects. Rapid deposition simultaneously produced silver films with a relatively large rms roughness of 4.32 nm. Silver was used as the gate electrode because of the ability to achieve high deposition rates, which resulted in relatively smooth films on the PLGA substrate. Gold films of similar thickness, deposited at a rate of 1 Å s^{-1} for 200 s, exhibited micrometer-scale roughness and precluded subsequent dielectric processing. However, gold was suitable for use in the source/drain contacts.

Thin-film transistors based on p-channel DDFTTF active layers and PVA dielectrics exhibited electron mobilities as high as 0.253 cm^2 s^{-1} V^{-1} and on/off current ratios (I_{on}/I_{off}) up to 9.4×10^3 (Table 1, Fig. 2). Devices fabricated on nPVA films exhibited generally enhanced performance compared to similar devices fabricated on xPVA dielectrics (Fig. S3). This includes enhanced mobility, increased I_{on}/I_{off}, and reduced threshold voltage (V_T; Table 1, $^{***}p < 0.001$ for all metrics). The origin of the effect on crosslinking PVA-dielectric films on resulting mobility is likely to be related to the alteration of the dielectric constant. The dielectric constants of nPVA and xPVA films, 7.6 and 6.7, respectively, were observed to be comparable with other solution-processed PVA films.[29–31] This reduction is, probably, due to the conversion of free hydroxyl groups into ether groups upon free-radical polymerization. Furthermore, this reduction is comparable to previous reports.[30,31] Other reports have demonstrated that even slight alterations in the dielectric constant can result in up to three-fold alterations in the mobility;[32] a similar span was roughly observed in this work. The pendant hydroxyl groups at the interface could serve as the primary reason for the reduced observed mobilities. Additionally, the hydroxyl groups at the PVA interface could also limit the ability to achieve saturation in the output characteristics of the device (Fig. 2), an effect that was observed in other devices that employ PVA as a dielectric material.[30] PVA dielectrics exhibited leakage currents on the order of 10^{-5} and $<10^{-5}$ A cm^{-2} at a gate-source voltage (V_{GS}) of −20 V for nPVA and xPVA films, respectively. These higher leakage currents could serve to reduce the maximum drain current and ultimately result in lower I_{on}/I_{off} than observed in

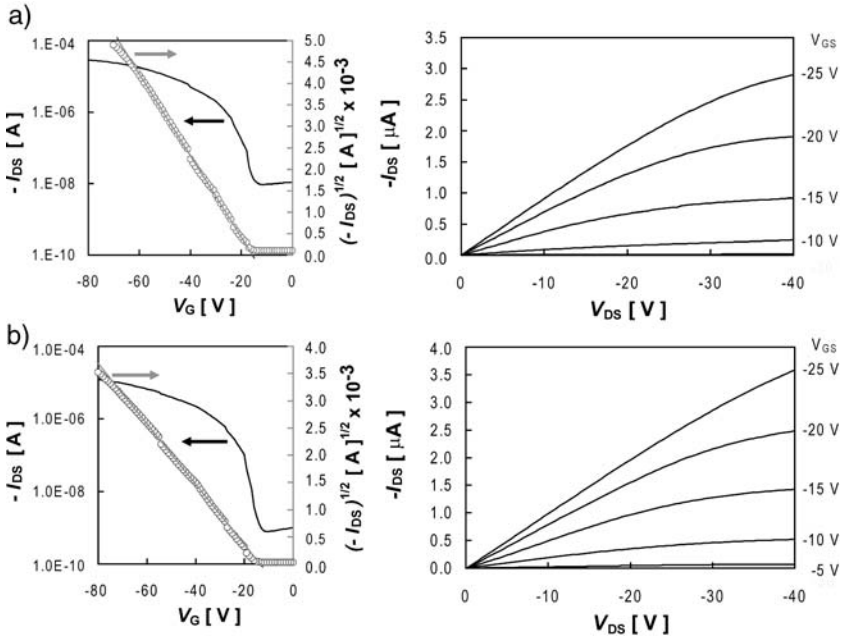

Figure 2. Electrical performance of representative DDFTTF-based transistors fabricated on PLGA substrates. Transistors fabricated from thermally evaporated DDFTTF semiconducting layers exhibited relatively high mobilities and on/off ratios on both (a) nPVA and (b) xPVA dielectrics. The device performance metrics for the device depicted in (a) are $\mu = 0.153\,cm^2\,s^{-1}\,V^{-1}$, $I_{on}/I_{off} = 3.49 \times 10^3$, and $V_T = -15.6\,V$. The device performance metrics for the device depicted in (b) are $\mu = 0.060\,cm^2\,s^{-1}\,V^{-1}$, $I_{on}/I_{off} = 2.93 \times 10^3$, and $V_T = -13.6\,V$.

previous reports that employed DDFTTF semiconducting channels.[17]

Future potential applications of these devices in biomedical or environmental applications presuppose the possibility of stable device operation after exposure to aqueous conditions. Transistors fabricated on xPVA dielectrics exhibited adequate performance after direct exposure of the semiconducting layer to liquid water for extended periods of time (Fig. 3). Exposure of the device to water led to reduced effective mobility (μ_{eff}), reduced I_{on}/I_{off}, and a shift in V_T from $\sim 18.9 \pm 4.9\,V$ to $2.82 \pm 7.3\,V$. Exposure of the DDFTTF semiconductor material led to a dramatic increase in the off current, which is likely due to high concentrations of hydroxide and hydronium ions entering the semiconductor/dielectric interface. Similar trends were also observed for exposure of DDFTTF on poly(4-vinyl-phenol) dielectrics.[17] It should be noted that exposure of the device to water using nPVA dielectrics resulted in immediate device failure due to delamination of the structure. Devices fabricated on both nPVA and xPVA substrates also immediately failed after exposure to phosphate buffered saline, which can probably be attributed to the high concentration of inorganic ionic species ($\sim$160 mM). The sensitivity of device performance to ionic species suggests that appropriate encapsulation and packaging of the device must be achieved before the possibility of utilizing this device in aqueous environments with high ion concentrations.

In vitro biodegradation studies were performed to investigate device resorption characteristics. Our primary goal was not to produce a device that would operate in the presence of a harsh environment. Rather, we wanted to show that these devices can indeed degrade under biological conditions. Exposing devices to citrate buffer led to the irreversible loss of device functionality in less than 2 days as the DDFTTF layer of the device delaminated from the dielectric. The mass-loss kinetics of the device, which is composed primarily of the PLGA substrate, was characterized thereafter (Fig. 4a). The mass-loss progression of devices fabricated on PLGA 85:15 substrates observed in this study was similar to that of previous studies of PLGA mass loss through hydrolysis mechanisms.[33–35] The devices were relatively resistant to mass loss and water uptake for $\sim$30 days. After this time, there was a significant decrease in mass and corresponding increase in hydration, as the device began to undergo rapid autocatalytic hydrolysis and bulk erosion. The observed degradation time scale was consistent with previous reports for this particular PLGA formulation.[33,36] The mass-loss kinetics exhibited a significant lag time, during which water infiltrated into the device, followed by rapid degradation. Significant mass loss and water uptake were observed thereafter. Structural integrity was lost at $\sim$50 days of degradation time, at which point the device was primarily composed of a viscous gel composed of low-molecular-weight PLGA (Fig. 4b).

Herein, we have described the design, fabrication, and characterization of water-stable organic thin film transistors fabricated using biodegradable and biocompatible polymers. These devices maintained functionality after direct exposure to water and are principally resorbable, as demonstrated through in vitro degradation studies. The potential utilization of resorbable organic electronics could serve as a motivating factor for the development of high-performance dielectrics and semiconducting molecules with the additional properties of biocompatibility and biodegradability into non-toxic and environmentally safe monomers. These degradation products could then be incorporated into metabolic pathways in order to undergo subsequent degradation steps. For example, recent work has examined the possibility of using DNA-based dielectrics for organic electronic applications.[37] Advanced encapsulation techniques will be required to enable in vivo operation of biodegradable electronic devices. Different biodegradable encapsulation materials may be designed to expand the operating conditions and control the rate of degradation of electronic as well as physical properties. Tailoring the packaging of these structures could also lead to preprogrammed device lifetimes by virtue of temporally mediating exposure of critical device components to caustic environments. The device functionality presented in this Communication is the first step towards realizing more complex biodegradable and compostable electronic devices. Subsequent design, fabrication, and integration of other simple electronic components fabricated from resorbable electronically active materials could be utilized in the realization of temporary medical implants with electronic functionality. For example, resorbable implants with electronic capability could be utilized as next-generation electroactive drug-delivery systems[38,39] or

Final page numbers not assigned

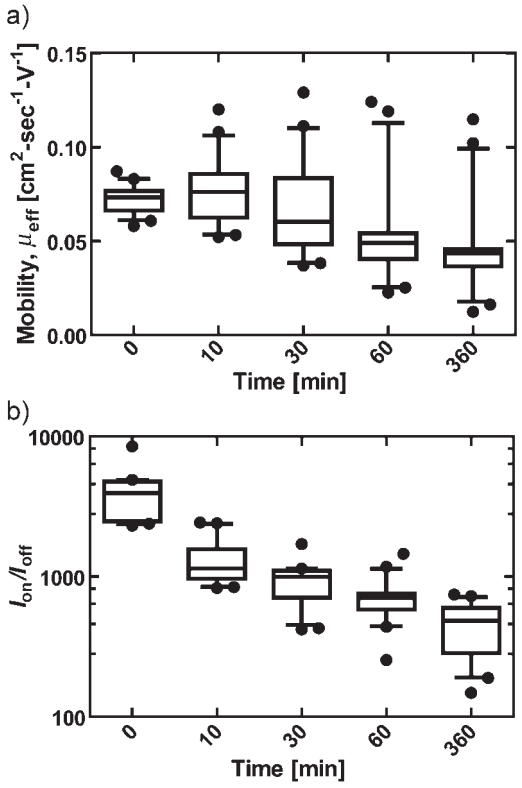

Figure 3. Effect of aqueous exposure on the device performance. The kinetics of electrical performance as a function of cumulative time exposed to ddH_2O is shown for a set of 20 devices. a) μ_{eff} was measured to decrease gradually over the course of 6 h. b) I_{on}/I_{off} was immediately reduced upon exposure to liquid water and then very gradually decreased over the remainder of the time course.

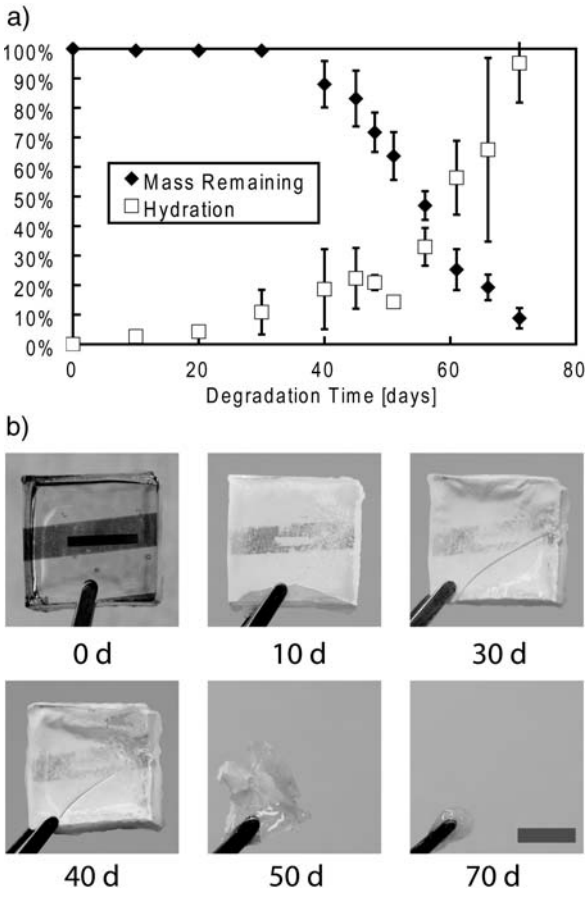

Figure 4. In vitro degradation of devices. a) A plot of mass remaining and water uptake by mass (hydration) demonstrates that devices fabricated on PLGA substrates were initially resistant to mass degradation and water uptake. However, after 30 days, significant mass loss and water uptake was initiated. Near-total mass loss and 100% device hydration was observed at 70 days. b) Photographs from representative devices at various stages of the degradation time line suggest that device integrity was intact up until 40 days with near-total device resorption at 70 days. Devices also show a transition from being initially optically transparent (0 days) to opaque within 10 day. Scale bar represents 5 mm for all panels.

tissue-engineering scaffolds.[40] Biodegradability could also be advantageous in utilizing compostable electronic devices in environmentally sensitive settings.

Experimental

Device Fabrication: All materials were used as received unless otherwise noted. PLGA (85:15, $M_w = 50000$–70000 Da, Sigma–Aldrich, St. Louis, MO, USA) was melted and cast into substrates with dimensions of ~1 cm × 1 cm × 2 mm (width (W) × length (L) × thickness (T)) using fluoropolymer-coated silicon substrates heated to ~200 °C using a hot plate. A conductive gate electrode was deposited by thermal evaporation of silver (Ag) through a shadow mask at 15–20 Å s^{-1} for 10 s to create a conductive film, 15–20 nm in thickness. PVA (Moliol 40–88, Sigma–Aldrich) solutions at a concentration of 10% (w/v) in double-distilled water (ddH_2O) were spin-coated to form the gate-dielectric layer. ADC (Sigma–Aldrich) was used as a photocrosslinking agent by dissolving into PVA solutions at a mass ratio of 1:6 ADC:PVA. Solutions were filtered using a 0.45 μm poly(vinylidene fluoride) filter (Millipore, Billerica, MA, USA) prior to spin-coating. PVA solutions were spin-coated onto substrates at 3000 rpm for 40 s. PVA films with ADC were photocrosslinked at $\lambda = 254$ nm for 10 min followed by rinsing with ddH_2O to remove residual ADC. All films underwent a dehydration bake at 50 °C for 18 h under 27 in. Hg vacuum. DDFTTF was chosen as the semiconductor for its stability in aqueous environments. DDFTTF was synthesized and purified as previously reported [17]. DDFTTF films were deposited by thermal evaporation (Angstrom Engineering, Kitchener, Ontario, Canada) at a rate of 0.2–0.4 Å s^{-1} under a pressure of 5.0×10^{-7} Torr. The temperature of the substrates was kept at 50 °C during deposition. Gold source/drain electrodes were thermally deposited through a shadow mask to form device channels 50 μm in length with a W/L ratio of 20.

Physical Device Characterization: PVA dielectric films were fabricated into metal–insulator–metal capacitors with gold as the top and bottom contacts. The film morphology was characterized by atomic force microscopy (AFM) (NanoScope IV, Digital Instruments, Plainview, NY, USA) operated in tapping mode (300 kHz frequency, Si tip). Film thicknesses were determined by profilometry (Dektak 150 Profilometer, Veeco, Plainview, NY, USA).

Electronic Device Characterization: The electrical measurements were carried out in ambient atmosphere by using a Keithley 4200SCS semiconductor parameter analyzer equipped with KITE Interactive and a standard probe-station setup. Values for μ and V_T were calculated by operating devices in the saturation regime and applying Equation (1), where I_{DS} is the source/drain current and C_d the dielectric capacitance.

$$|I_{DS}| = \mu C_d \frac{W}{2L}(V_{GS} - V_T)^2 \quad (1)$$

C_d measurements were performed by using a Hewlett–Packard 4192 LF Impedance Analyzer for frequencies ranging between 20 Hz and 100 KHz. Samples Unpaired student's *t*-tests were performed where appropriate with significance values set at $*p < 0.05$, $**p < 0.01$, and $***p < 0.001$ (GraphPad Prism, La Jolla, CA, USA). All values are reported as mean ± standard deviation (sd) unless stated otherwise. Box-whisker plots indicate lower and upper quartiles with a 10–90% confidence interval, respectively. Outliers beyond this range are shown as discrete points. At least 60 devices were characterized for dry-performance characteristics and at least 20 devices were characterized at each time point for water-exposure experiments.

Degradation Studies: Devices with xPVA dielectrics were dedicated for biodegradation studies ($n = 4$) and were incubated in citrate buffer (pH = 4.0) at 37 °C. Macroscopic photos were taken with an Olympus E520 camera. Devices were removed at predetermined time points, washed with ddH_2O, pat dried, and weighed to obtain the mass of wet devices, $m_{wet}(t)$. Samples were then dried under vacuum for 4 days at 35 °C to remove all moisture and the devices were measured again to obtain $m_{dry}(t)$. Mass loss and device hydration were determined from Equation (2) and (3), respectively.

$$m_{Loss}(t) = \frac{m_{dry}(t) - m_{dry}(t_o)}{m_{dry}(t_o)} \quad (2)$$

$$m_{Hyd}(t) = \frac{m_{wet}(t) - m_{dry}(t)}{m_{dry}(t)} \quad (3)$$

where $m(t)$ is the mass at a given time t and $m(t_o)$ is the initial mass.

Acknowledgements

The authors acknowledge Debbie Lin and Anatoly Sokolov for assistance in sample preparation and instrumentation. Financial support for this project was provided by the National Institutes of Health (grant no. 1F32NS064771-01) and the Office of Naval Research (N000140810654) MURI project. C.J.B. was funded by a Ruth L. Kirschstein NIH fellowship. Supporting Information is available online from Wiley InterScience or from the author.

Received: July 11, 2009
Revised: August 24, 2009
Published online:

[1] M. E. Roberts, S. C. B. Mannsfeld, R. M. Stoltenberg, Z. Bao, *Org. Electron.* **2009**, *10*, 377.
[2] A. L. Briseno, R. J. Tseng, M. M. Ling, E. H. L. Falcao, Y. Yang, F. Wudl, Z. Bao, *Adv. Mater.* **2006**, *18*, 2320.
[3] J. A. Rogers, Z. Bao, K. Baldwin, A. Dodabalapur, B. Crone, V. R. Raju, V. Kuck, H. Katz, K. Amundson, J. Ewing, P. Drzaic, *Proc. Natl. Acad. Sci. U S A* **2001**, *90*, 4835.
[4] T. Someya, Y. Kato, T. Sekitani, S. Iba, Y. Noguchi, Y. Murase, H. Kawaguchi, T. Sakurai, *Proc. Natl. Acad. Sci. USA* **2005**, *102*, 12321.
[5] G. P. Kushto, W. Kim, Z. H. Kafafi, *Appl. Phys. Lett.* **2005**, *86*, 093502.
[6] E. Fortunato, N. Correia, P. Barquinha, L. Pereira, G. Goncalves, R. Martins, *IEEE Elect. Dev. Lett.* **2008**, *29*, 988.
[7] K. Yong-Hoon, M. Dae-Gyu, H. Jeong-In, *IEEE Elect. Dev. Lett.* **2004**, *25*, 702.
[8] D.-H. Kim, Y.-S. Kim, J. Amsden, B. Panilaitis, D. L. Kaplan, F. G. Omenetto, M. R. Zakin, J. A. Rogers, *Appl. Phys. Lett.* **2009**, *95*, 133701.
[9] R. A. Gross, B. Kalra, *Science* **2002**, *297*, 803.
[10] H. Tamai, K. Igaki, E. Kyo, K. Kosuga, A. Kawashima, S. Matsui, H. Komori, T. Tsuji, S. Motohara, H. Uehata, *Circulation* **2000**, *102*, 399.
[11] J. C. Middleton, A. J. Tipton, *Biomaterials* **2000**, *21*, 2335.
[12] I. Paetau, C. Z. Chen, J. Jane, *J. Polym. Environ.* **1994**, *2*, 211.
[13] D. P. Martin, S. F. Williams, *Biochem. Eng. J.* **2003**, *16*, 97.
[14] L. S. Ferreira, S. Gerecht, J. Fuller, H. F. Shieh, G. Vunjak-Novakovic, R. Langer, *Biomaterials* **2007**, *28*, 2706.
[15] E. Chiellini, A. Corti, S. D'Antone, R. Solaro, *Prog. Polym. Sci.* **2003**, *28*, 963.
[16] A. B. Mallik, J. Locklin, S. C. B. Mannsfeld, C. Reese, M. E. Roberts, M. L. Senatore, H. Zi, Z. Bao, in: *Organic Field Effect Transistors*, (Eds.: Z, Bao, J. Locklin), CRC Press, Boca Raton, FL USA **2007**, pp. 159–228.
[17] M. E. Roberts, S. C. B. Mannsfeld, N. Queraltó, C. Reese, J. Locklin, W. K. Z. Bao, *Proc. Natl. Acad. Sci. USA* **2008**, *105*, 12134.
[18] J. Locklin, M. M. Ling, A. Sung, M. E. Roberts, Z. Bao, *Adv. Mater.* **2006**, *18*, 2989.
[19] J. H. Oh, S. Liu, Z. Bao, R. Schmidt, F. Wurthner, *Appl. Phys. Lett.* **2007**, *91*, 212107.
[20] J. McGinness, P. Corry, P. Proctor, *Science* **1974**, *183*, 853.
[21] A. Napolitano, A. Pezzella, M. R. Vincensi, G. Prota, *Tetrahedron* **1995**, *51*, 5913.
[22] S. Ito, *Pigm. Cell Res.* **2003**, *16*, 230.
[23] C. J. Bettinger, J. P. Bruggeman, A. Misra, J. T. Borenstein, R. Langer, *Biomaterials* **2009**, *30*, 3050.
[24] M. Bosetti, A. Massè, E. Tobin, M. Cannas, *Biomaterials* **2002**, *23*, 887.
[25] A. Massè, A. Bruno, M. Bosetti, A. Biasibetti, M. Cannas, P. Gallinaro, *J. Biomed. Mater. Res. B* **2000**, *53*, 600.
[26] E. R. Edelman, P. Seifert, A. Groothuis, A. Morss, D. Bornstein, C. Rogers, *Circulation* **2001**, *103*, 429.
[27] G. Voskerician, M. S. Shive, R. S. Shawgo, H. v, Recum, J. M. Anderson, M. J. Cima, R. Langer, *Biomaterials* **2003**, *24*, 1959.
[28] S. H. Kim, S. Y. Yang, K. Shin, H. Jeon, J. W. Lee, K. P. Hong, C. E. Park, *Appl. Phys. Lett.* **2006**, *89*, 183516.
[29] A. Maliakal, in: *Organic Field Effect Transistors*, (Eds.: Z, Bao, J. Locklin), CRC Press, Boca Raton, FL USA **2007**, pp. 229–251.
[30] S. H. Jin, J. S. Yu, C. A. Lee, J. W. Kim, B.-G. Park, J. D. Lee, *J. Korean Phy. Soc.* **2004**, *44*, 181.
[31] T. B. Singh, F. Meghdadi, S. Gunes, N. Marjanovic, G. Horowitz, P. Lang, S. Bauer, N. S. Sariciftci, *Adv. Mater.* **2005**, *17*, 2315.
[32] Y. Jang, D. H. Kim, Y. D. Park, J. H. Cho, M. Hwang, K. Choa, *Appl. Phys. Lett.* **2005**, *87*, 152105.
[33] L. Lu, C. A. Garcia, A. G. Mikos, *J. Biomed. Mater. Res.* **1999**, *46*, 236.
[34] C. J. Bettinger, J. P. Bruggeman, J. T. Borenstein, R. S. Langer, *Biomaterials* **2008**, *29*, 2315.
[35] Y. Wang, Y. M. Kim, R. Langer, *J. Biomed. Mater. Res. A* **2003**, *66*, 192.
[36] L. Lu, S. J. Peter, M. D. Lyman, H.-L. Lai, S. M. Leite, J. A. Tamada, S. Uyama, J. P. Vacanti, L. Robert, A. G. Mikos, *Biomaterials* **2000**, *21*, 1837.
[37] P. Stadler, K. Oppelt, T. B. Singh, J. G. Grote, R. Schwödiauer, S. Bauer, H. Piglmayer-Brezina, D. Bäuerle, N. S. Sariciftci, *Org. Electron.* **2007**, *8*, 648.
[38] J. H. Prescott, S. Lipka, S. Baldwin, N. F. Sheppard, J. M. Maloney, J. Coppeta, B. Yomtov, M. A. Staples, J. T. Santini, *Nat. Biotechnol.* **2006**, *24*, 437.
[39] J. T. Santini, M. J. Cima, R. Langer, *Nature* **1999**, *397*, 335.
[40] M. Radisic, H. Park, H. Shing, T. Consi, F. J. Schoen, R. Langer, L. E. Freed, G. Vunjak-Novakovic, *Proc. Natl. Acad. Sci. U S A* **2004**, *101*, 18129.